Preprint typeset using LaTeX style emulateapj

AN EXCESS OF SUBMM SOURCES NEAR 4C 41.17: A CANDIDATE PROTO-CLUSTER AT Z=3.8?

R. J. IVISON,[1,2] J. S. DUNLOP,[3] IAN SMAIL,[4,5] ARJUN DEY[6], MICHAEL C. LIU[7] & J. R. GRAHAM[7]

1) Department of Physics & Astronomy, University College London, Gower Street, London WC1E 6BT, UK

3) Institute for Astronomy, University of Edinburgh, Blackford Hill, Edinburgh EH9 3HJ, UK

4) Department of Physics, University of Durham, South Road, Durham DH1 3LE, UK

6) NOAO, 950 N. Cherry Ave, Tucson AZ 85719

7) Astronomy Department, University of California at Berkeley, CA 94720

Received: 2000 March 26; accepted 2000 May 9

ABSTRACT

Biased galaxy-formation theories predict that massive galaxies at high redshifts should act as signposts to high-density environments in the early universe, which subsequently evolve into the cores of the richest clusters seen at the present day. These regions are characterised by over-densities of young galaxies, perhaps including a population of dusty, interaction-driven starbursts — the progenitors of massive cluster ellipticals. By searching for this population at submillimeter (submm) wavelengths we can therefore test both galaxy- and structure-formation models. We have undertaken such a search in the field of a $z = 3.8$ radio galaxy, 4C 41.17, with the SCUBA submm camera. Our extremely deep 450- and 850-μm maps reveal an order-of-magnitude over-density of luminous submm galaxies compared to typical fields (the likelihood of finding such an over-density in a random field is $< 2 \times 10^{-3}$). The SCUBA galaxies have bolometric luminosities, $> 10^{13}\,L_{\odot}$, which imply star-formation rates (SFRs) consistent with those required to form a massive galaxy in only a few 10^8 years. We also note that this field exhibits an over-density of extremely red objects (EROs), some of which may be associated with the submm sources, and Lyman-break galaxies. We propose that the over-densities of both submm and ERO sources in this field represent young dusty, starburst galaxies forming within a proto-cluster centered on the radio galaxy at $z = 3.8$, which is also traced by a less-obscured population of Lyman-break galaxies.

Subject headings: cosmology: observations — galaxies: evolution — galaxies: formation — infrared: galaxies — radio: galaxies

1. INTRODUCTION

Galaxy-formation theories are developing rapidly and have claimed some success at reproducing the properties of galaxies in the local universe (Cole et al. 1994). However, at the moment their predictions of the early evolution of galaxies are comparatively untested. Moreover, the areas where the theoretical predictions are most reliable tend to be those where the observational tests are most difficult at high redshift, e.g., the evolution in the mass function of galaxies (White & Frenk 1991). One testable prediction of hierarchical galaxy-formation models at high redshifts deals with the clustering behaviour of massive galaxies at early epochs: such galaxies are expected to cluster strongly in regions of highest density, areas which should subsequently form the cores of massive clusters of galaxies in the local universe (Kaiser 1984; Baron & White 1987; Efstathiou & Rees 1988; Kauffmann et al. 1999). Thus by searching for over-densities of massive galaxies in the distant universe we can test the predictions of hierarchical models *as well as* investigating the formation and evolution of the luminous galaxies seen in present-day clusters. However, to achieve this we must find a method of selecting the densest regions in the early universe.

One possible technique is to use massive galaxies as signposts for high-density environments at high redshifts. Observations of distant, luminous radio galaxies have led to the suggestion that they are massive ellipticals (Matthews, Morgan & Schmidt 1964; Lilly & Longair 1984), a belief confirmed recently by *Hubble Space Telescope* (*HST*) studies which show they possess $r^{1/4}$-law profiles characteristic of elliptical galaxies (McLure et al. 1999; Zirm et al. 2000). Locally these massive elliptical galaxies typical reside in galaxy clusters and hence luminous radio galaxies should make good markers to search for the progenitors of rich galaxy clusters at high redshifts.

The picture of hierarchical formation of massive galaxies and their environments is supported on small scales by recent rest-frame optical imaging of radio galaxies (van Breugel et al. 1998; Pentericci et al. 1998): at the earliest epochs ($z \geq 4$) there is evidence of diffuse emission on large scales (5–10$''$) and subclumps similar in scale (~ 10 kpc) to radio-quiet star-forming galaxies; these then appear to evolve into more compact structures by $z \sim 2$. Interestingly, on somewhat larger scales there is also an apparent 10–100-fold increase in the surface density of EROs — some of which are dusty, star-forming galaxies akin to local ULIRGs (Dey et al. 1999; Smail et al. 1999) — around high-redshift radio galaxies (HzRGs) and quasars as compared with the field (Hu & Ridgway 1994; Elston, Rieke & Rieke 1988; Aragón-Salamanca et al. 1994; Dey, Spinrad & Dickinson 1995; Yamada et al. 1997). On similar scales, the distorted radio morphologies and high rotation measures of some HzRGs suggest they reside in high-density environments (Carilli et al. 1997) with extended X-ray emission detected around one example, 1138–262 at $z = 2.2$ (Carilli et al. 1998).

Confirming that HzRGs reside in high-density environments would also provide substantial insight into galaxy evolution in these regions, especially the formation of giant ellipticals in the hierarchical models already discussed. Optical/IR studies have

[2]PPARC Advanced Fellow.

[5]Royal Society University Research Fellow.

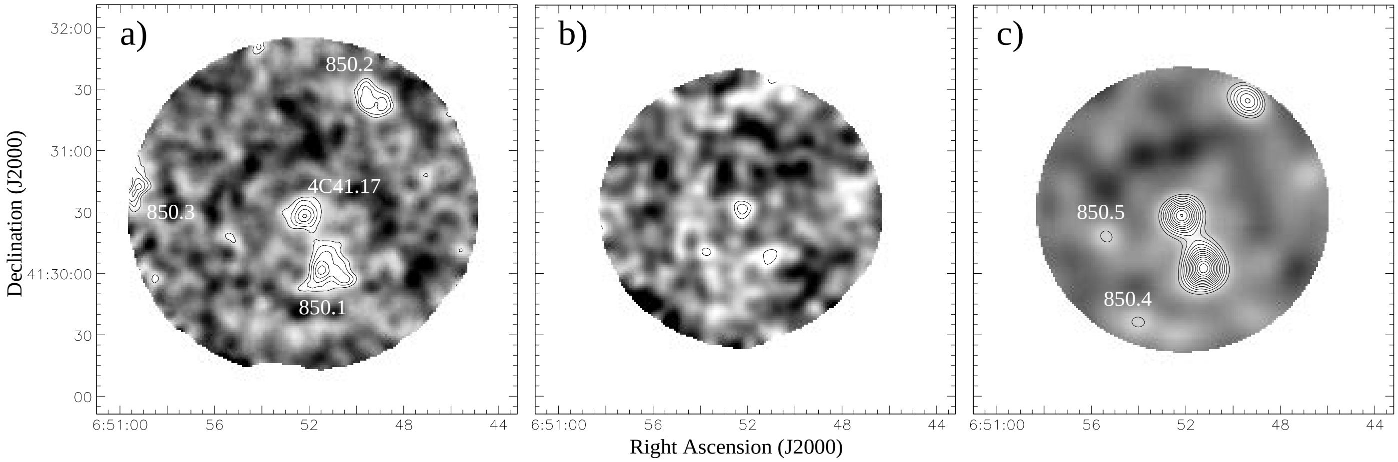

FIG. 1.—a) Full 850-μm image of the z = 3.8 radio galaxy, 4C 41.17, at the original $\sim 14''$ resolution. Negative features are due to the chopped/nodded observing procedure. Contours are plotted at $3, 4, 5, 6, 7 \times 1.5$ mJy beam^{-1}. b) 450-μm image of 4C 41.17, smoothed to a resolution of $10''$ FWHM. Contours are plotted at $3, 4 \times 8.6$ mJy per $10''$ beam^{-1}. c) Central, cleaned portion of the 850-μm image. Contours are plotted at $3, 4 \ldots 15 \times 0.8$ mJy beam^{-1}, where the beam has been smoothed to $20''$ in the background regions.

targeted the evolution of ellipticals in clusters at $z < 1$ (Aragón-Salamanca et al. 1993; Stanford, Eisenhardt & Dickinson 1998; Bower, Lucey & Ellis 1992; Ellis et al. 1997); theoretical work has investigated their evolution in the context of hierarchical formation in high-density regions (Kauffmann & Charlot 1998; Baugh et al. 1999). Pinpointing the progenitors of ellipticals at very high redshifts would allow straightforward tests of the latter models and would enable the time-line of the optical/IR cluster studies to be extended beyond $z \sim 1.3$ (Stanford et al. 1997, 1998; Rosati et al. 1999; Liu et al. 2000).

In the hierarchical picture, lower-mass structures will accrete onto the high-mass peak of the proto-cluster identified with the radio galaxy, the final assembly of this structure achieved through a series of mergers which will strongly affect the galaxies residing within the dark matter halo, triggering intense starbursts analogous to mergers in the local universe (Sanders & Mirabel 1996). The dust created in these starbursts will absorb a considerable fraction of the UV/optical light emitted by young stars, re-emitting it in the rest-frame far-IR. An extreme and highly obscured starburst with a SFR of $\sim 1000\,\mathrm{M_\odot yr^{-1}}$ would have a bolometric luminosity, $L_{\rm bol}$, of $\sim 10^{13}\,\mathrm{L_\odot}$, and the majority of this would appear at rest-frame far-IR wavelengths (Ivison et al. 1998).

The negative K-correction for dust emission in the submm passband (Blain & Longair 1993) means that a luminous, dusty starburst with $L_{\rm bol} \sim 10^{13}\,\mathrm{L_\odot}$ would have an 850-μm flux of ~ 10 mJy if observed at *any* redshift between 1 and 10. The advent of sensitive arrays working at submm wavelengths, in particular the SCUBA camera (Holland et al. 1999) on the James Clerk Maxwell Telescope (JCMT) have enabled efficient and sensitive surveys of dusty starbursts, probing out to high redshifts (Smail, Ivison & Blain 1997; Barger et al. 1998; Hughes et al. 1998; Eales et al. 1999).

Thus by using SCUBA to undertake targeted observations of the environments of known HzRGs, searching for over-densities of bright submm sources, we can test whether HzRGs are located in the cores of rich proto-clusters *and* constrain the formation epoch of massive cluster galaxies. For targets at $z \gtrsim 2$ the resolution and field of view of SCUBA at 850 μm means we are sensitive to star-forming galaxies distributed on scales from 100 to 1000 kpc — well-matched to the predicted virial radii of the most massive clusters at these epochs (Jenkins et al. 2000).

In this paper we present deep 450- and 850-μm maps of one of the most distant and powerful known radio galaxies, 4C 41.17 at z = 3.8 (for which $1''$ = $6.6\,h_{50}^{-1}$ kpc, with h_{50} = $H_0/50\,\mathrm{km\,s^{-1}\,Mpc^{-1}}$ and $q_0 = 0.5$). There is already some evidence for a massive structure associated with 4C 41.17. Based upon a Lyman-break search using *UVR* imaging, Lacy & Rawlings (1996) have suggested that there is a modest excess of high-redshift galaxies in this region, having found six candidate $z \gtrsim 3.4$ galaxies in a 1.5-arcmin^2 field, roughly centered on 4C 41.17. They show that this density is slightly higher than that expected from the field density found by Steidel, Pettini & Hamilton (1995), but the complications introduced by comparing their *UVR* study with Steidel et al.'s $\mathcal{UGR}$ survey, as well as issues of cosmic variance (Steidel et al. 1999), make it difficult to assess the over-density. Other evidence for a deep potential centered on the radio galaxy includes the presence of an extended Lyα halo reaching to $>$100 kpc (Chambers, Miley & van Breugel 1990; Dey 1999).

In the next section we present our submm, near-IR and optical observations of this field and their reduction. We discuss our analysis and results, in the context of supporting archival data at other wavelengths, in §3 and give our conclusions in §4.

2. OBSERVATIONS AND DATA REDUCTION

2.1. *Submillimeter Observations*

During 1998 October we used SCUBA to map a $\sim 2.5'$-diameter field at 450- and 850-μm, centred on 4C 41.17 (Fig. 1). The secondary mirror followed a jiggle pattern designed to fully sample the image plane, chopping by $45''$ between the 'on' and 'off' positions at 7 Hz whilst the telescope nodded between the same positions every 16 s in an on–off–off–on pattern. The chop throw was chosen to optimise calibration accuracy, minimise noise, maximise regions for which both 'on' and 'off' beam information would be available, and minimise the possibility of bright sources close to the field of view contaminating the map. Two directions were used for the chopping: north–south (N–S) as the target rose and set; east-west (E–W) when the target was near transit. This method ensured the chop direction was close to azimuthal whilst retaining the advantages of on-array chopping. It also provided independent maps which could be cleaned separately and coadded, reducing the risk of spurious detections and of chopping consistently from one source onto another.

The sky was exceptionally stable and transparent for the five

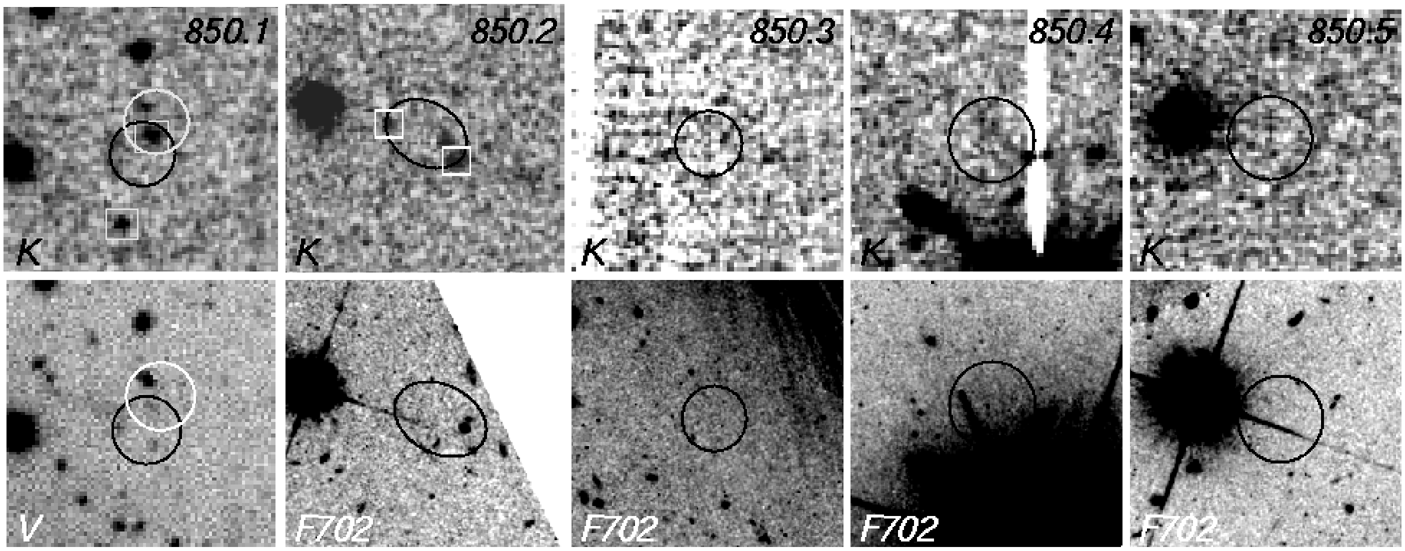

FIG. 2.— KPNO 2.1-m K'-band imaging and *HST* F702W images of $25'' \times 25''$ regions around the submm sources, smoothed with $0.5''$- and $0.15''$-FWHM Gaussians at K' and $F702W$ respectively. For HzRG850.1, the optical data are from Keck II (§2.2). EROs are marked with squares; 850-μm positions are marked with $6''$- or $8''$-diameter black circles (an ellipse for HzRG850.2); the 450-μm position of HzRG850.1 is marked with a white circle.

nights during which data were obtained. The total exposure time was 36 ks and the opacity at 850 μm, measured every hour, was typically 0.15–0.20, never rising above 0.25. Flux calibration was accomplished using beam maps of Mars. Nightly calibration factors were stable: consistent at the 5% level (r.m.s.) at 850 μm. Even at 450 μm, factors were stable at the 10% level. Absolute flux calibration should be accurate to $\sim$ 10%.

Maps were created using SURF (Jenness & Lightfoot 1997). In order to extract reliable source positions and flux densities, the images (Fig. 1) and the symmetric $-1,+2,-1$ zero-flux beam (which arises from chopping and nodding) were deconvolved using a modified version of the CLEAN algorithm (Hogbom 1974) as follows. The E–W- and N–S-chopped maps were treated separately for the purpose of deconvolution. First, both the image and the appropriate beam (from contemporaneous maps of blazars) were convolved with a Gaussian (FWHM $14''$, similar to the core of the JCMT beam at 850 μm). The smoothed image was then cleaned using the smoothed beam, down to a level equivalent to twice the r.m.s. noise of the smoothed data, using a loop-gain of 0.1. This has the effect of gradually removing the positive core of a real source from the data, while at the same time filling in its negative sidelobes. When the process is complete, the original image is reduced to a map of background noise (still containing real sources which are too faint to have been identified as significant peaks by the CLEAN algorithm) while the absolute values of removed flux are stored as a set of delta functions (in the case of unresolved sources) located at the positions of the original source peaks.

The restored images were produced by halving the size of the delta functions then convolving them with a Gaussian (FWHM $14''$) and adding them back into the residual noise image left by the cleaning process. The result is a restored image with the angular resolution of the original but free from negative sidelobes associated with significant sources. One advantage of this process is that it should resurrect any significant sources whose flux has been depressed (or annihilated) because they happen to lie in the negative sidelobe of another source, though only sources within $70''$ of the field centre are treated properly by the cleaning procedure. Sources which were produced in both the E–W- and N–S-chopped, restored sub-images, with positions differing by less than $3''$, can be regarded as robust detections.

2.2. *Near-Infrared and Optical Observations*

We used the Ohio State/NOAO IR Spectrometer (ONIS) on the 2.1-m telescope of the Kitt Peak National Observatory to obtain K-band images of the 4C 41.17 field covering a $5.6' \times 8.0'$ field at $0.34''$/pixel sampling. The observations were taken in $0.9''$ seeing on the nights of 1998 November 14, 15 and 1999 March 20. Observations were made using a random dither pattern, with multiple 60 s integrations at each pointing and a combined exposure time of 16.3 ks. The data were dark subtracted, linearized, flat fielded, and the final mosaic (Fig. 2) was constructed using a modified version of DIMSUM in IRAF[8]. The photometric calibration was accomplished using observations of several *HST* IR standard stars (Persson et al. 1998) and checked against the photometry of Graham et al. (1994) for the sources in common. The images were astrometrically calibrated using the U.S. Naval Observatory A2.0 Catalog. The final K-band mosaic has a seeing FWHM of $1.0''$ and reaches a 5σ limit of K = 19.2 in a $2''$ diameter aperture.

In addition to these wide-field observations, we also obtained deep JHK images of the fields of two of the brighter SCUBA sources (HzRG850.1 and HzRG850.2; see below) using the Near-IR Camera (NIRC, Matthews & Soifer 1994) at the W. M. Keck Observatory in photometric conditions on the nights of 1999 March 24 and 25. NIRC has a $38''$ field of view with $0.15''$/pixel sampling and the observations were taken with a random dither pattern, with a 120-s exposure per pointing. Over the two nights, we obtained total integrations on HzRG850.1 of 1.2 ks, 2.4 ks and 1.2 ks in JHK respectively, with 2.4 ks, 1.2 ks and 2.4 ks in JHK on the HzRG850.2 field. The frames were reduced and combined in a standard manner and we show the resulting composite color images in Fig. 3. The seeing measured off the final stacked frames is 0.5–$0.6''$and the frames were calibrated using the faint standards from Persson et al. (1998) yielding detection limits of $J \sim 24$, $H \sim 22.5$ and $K \sim 21$.

V-band images of the 4C 41.17 field were obtained using the Low Resolution Imaging Spectrometer (LRIS; Oke et al. 1995) on Keck II on 1998 September 19. The total exposure time was

[8] IRAF is distributed by the National Optical Astronomy Observatories.

2.7 ks, broken into 9 dithered sub-exposures. Conditions were non-photometric, but the data were calibrated using magnitudes of objects in the field from Lacy & Rawlings (1996). The final image reaches a 5σ limiting magnitude of $V = 26.3$ in a $2''$ diameter aperture.

Finally, we have also made use of the archival *HST* WFPC2 image of this field (GO#5511). This comprises a total of 21.6 ks integration through the F702W filter and reaches a 3-σ limiting magnitude of $R = 26.0$ ($2''$ aperture, converted to Cousins R using photometry of sources with $R-K \sim 4$ in Graham et al. 1994).

These combined optical and near-IR observations identify several new ERO sources to add to the two originally found by Graham et al. (1994). In total we identify at least five objects with extreme colors, $R-K \geq 6$ or $V-K \geq 7$, brighter than $K = 20$ within roughly a 2 arcmin^2 field. This surface density is nearly an order of magnitude higher than that seen in blank fields (e.g. Thompson et al. 1999) and as we discuss below several of these objects maybe associated with the submm sources in this field.

3. RESULTS AND DISCUSSION

3.1. *Submillimeter sources*

At 850 μm, the cleaned portion of the map (4.3 arcmin^2) reaches a 4-σ sensitivity of 3.2 mJy beam^{-1} (6.0 mJy beam^{-1} for a further 1.6 arcmin^2), sufficient to detect galaxies with SFRs of a few 100 $M_\odot$ yr^{-1} at the redshift of 4C 41.17.

In the cleaned image we detect three sources well above the 4-σ flux limit with positions differing by $< 3''$ in the sub-images (Table 1); of these, one is associated with the radio galaxy, as determined previously by Dunlop et al. (1994). The others are new detections and one of them, HzRG850.1, is the brightest 850-μm source yet reported. As we discuss in §3.2, this represents a large over-density compared to the expected blank-field count of 0.1–0.3 per SCUBA field.

TABLE 1
POSITIONS AND FLUX DENSITIES OF SUBMM SOURCES

IAU name	RA[a] (h min s ± s)	Dec.[a] (° ′ ″ ± ″)	$S^{b}_{850\mu m}$ (mJy)	$S^{b}_{450\mu m}$ (mJy)
HzRG850.1[c]	06 50 51.2 ± 0.3	+41 30 05 ± 3	15.6 ± 1.8	34.1 ± 9.3
	06 50 51.0 ± 0.3[d]	+41 30 08 ± 3[d]		
HzRG850.2[c]	06 50 49.3 ± 0.4	+41 31 27 ± 3	8.7 ± 1.2	—[e]
HzRG850.3[f]	06 50 59.3 ± 0.4	+41 30 45 ± 3	6.5 ± 1.6	—[e]
4C 41.17[c]	06 50 52.14	+41 30 30.8	11.0 ± 1.4	35.3 ± 9.3
HzRG850.4	06 50 54.0 ± 0.4	+41 29 39 ± 4	2.8 ± 0.8	$3\sigma < 26$
HzRG850.5	06 50 55.3 ± 0.4	+41 30 20 ± 4	2.4 ± 0.8	$3\sigma < 26$

NOTES: *a*) 850-μm position (J2000); *b*) Photometry measurements, taking the $15''$-diameter aperture-corrected value at 850 μm and the $7.5''$-diameter aperture-corrected value at 450 μm; errors include a 10% contribution from the uncertainty in absolute flux calibration; *c*) Positions and fluxes were measured from the cleaned image. The 850-μm maps were shifted $0.3''$ west, $2.4''$ north ($1.0''$ west, $0.4''$ south for the 450-μm map) such that the submm emission from 4C 41.17 coincided with the radio core; *d*) 450-μm position; *e*) Source lies off the 450-μm map; *f*) Lies outside of $70''$-radius cleaned zone.

The flux measurements of HzRG850.1 (Table 1) suggest that it is resolved. Aperture-corrected fluxes (based on Mars, with a $4.5''$ diameter) increase with aperture size, showing a 50% increase in flux when going from a $5''$- to a $15''$-diameter aperture. This indicates that HzRG850.1 subtends $> 4.5''$, consistent with the result of deconvolving it from the best-fit Gaussian profile for the instrumental beam which suggests a FWHM of $\sim 10''$. The 850-μm emission from 4C 41.17 and HzRG850.2 may also be resolved; their beam-corrected FWHM are $\sim 7''$ and $\sim 2''$ respectively.

Two other 850-μm sources are also *marginally* detected ($\geq 3\sigma$) in the cleaned map (one of these is also seen in the uncleaned map) and one further source is detected towards the eastern edge of the larger, uncleaned map: it reaches 6σ at its peak and it is seen in the E–W- and N–S-chopped sub-images so we consider it a robust detection, though its proximity to the map edge means that caution should be exercised regarding its precise flux and position (again, see Table 1).

Of the four robust 850-μm sources, two are also detected at 450 μm: HzRG850.1 and 4C 41.17. The positional coincidence with the 850-μm sources leaves little doubt of their reality, whilst the low flux levels indicate high redshifts. HzRG850.2 is not detected, although it lies on the extreme edge of the 450-μm map. Neither of the two marginal 850-μm sources are detected at 450 μm, and the bright eastern source does not lie on the 450-μm map. One further faint (3σ) source appears in the 450-μm map; it has no counterpart at 850 μm.

3.2. *Source counts and clustering*

Clearly, this field shows startling evidence for extremely luminous submm galaxies, possibly in a structure associated with the radio galaxy, 4C 41.17 at $z = 3.8$. We first discuss the strength of this over-density and the evidence for excesses of other classes of proposed high-redshift galaxies in this field, before going on to examine the available information on the redshifts of the submm galaxies to determine if it is consistent with them lying at the same redshift as 4C 41.17 and hence whether they can be placed in the heart of the proposed proto-cluster.

How does the submm galaxy density towards 4C 41.17 compare with that expected in blank-fields (Smail et al. 1997; Hughes et al. 1998; Barger et al. 1999; Blain et al. 1999; Eales et al. 1999)? *Excluding* 4C 41.17, the density of $S(850\,\mu\mathrm{m}) \geq 8$-mJy sources is 1220 ± 860 deg^{-2}; the weighted mean 8-mJy blank-field count is an order of magnitude lower at 134 ± 57 deg^{-2}. Delving slightly deeper, $S(850\,\mu\mathrm{m}) \geq 6.5$-mJy is 1830 ± 860 deg^{-2} versus 303 ± 108 deg^{-2} in blank fields. The observed source density at $S(850\,\mu\mathrm{m}) \geq 8$-mJy in the 4C 41.17 is equal to that seen in blank fields at a flux limit of only $S(850\,\mu\mathrm{m}) \sim 2.5$ mJy, below our 4σ detection threshold.[9]

Adopting the standard probabilistic methodology used in studies of clustering and confusion (e.g. Lilly et al. 1999), it is a simple exercise to determine the likelihood, P, of detecting so many bright sources within the 4C 41.17 field: $P < 0.00166$, meaning that on average we would have to observe more than 600 typical blank fields before finding a configuration of the type seen towards 4C 41.17. Note that P is given as an upper limit because HzRG850.1 is the brightest known 850-μm source and $S(850\,\mu\mathrm{m}) \geq 15$ mJy is thus unknown; we conservatively adopt $[S(850\,\mu\mathrm{m}) \geq 15\,\mathrm{mJy}] = [S(850\,\mu\mathrm{m}) \geq 8\,\mathrm{mJy}]$.

We note that the integrated 850-μm flux density in sources brighter than 2 mJy in this field is $\sim 3.3 \times 10^{-10}$ W m^{-2} sr^{-1}, so we have resolved $\gtrsim 90\%$ of the expected extragalactic background in the submm, based on its detection by *COBE* (Fixsen et al. 1998), and would far exceed it by ~ 1 mJy.

3.3. *Counterparts*

Before discussing the optical and near-IR counterparts to the submm sources around 4C 41.17, we introduce a nomenclature

[9] This allows us to rule out the alternative suggestion that the high density of submm galaxies results from amplification bias due to a foreground mass structure, which also amplifies the radio source. To achieve the necessary amplification across the SCUBA field ($A \sim 3$), the lens would have to have a mass of $\sim 10^{15} M_\odot$ within the field – such a massive foreground cluster would be easily visible.

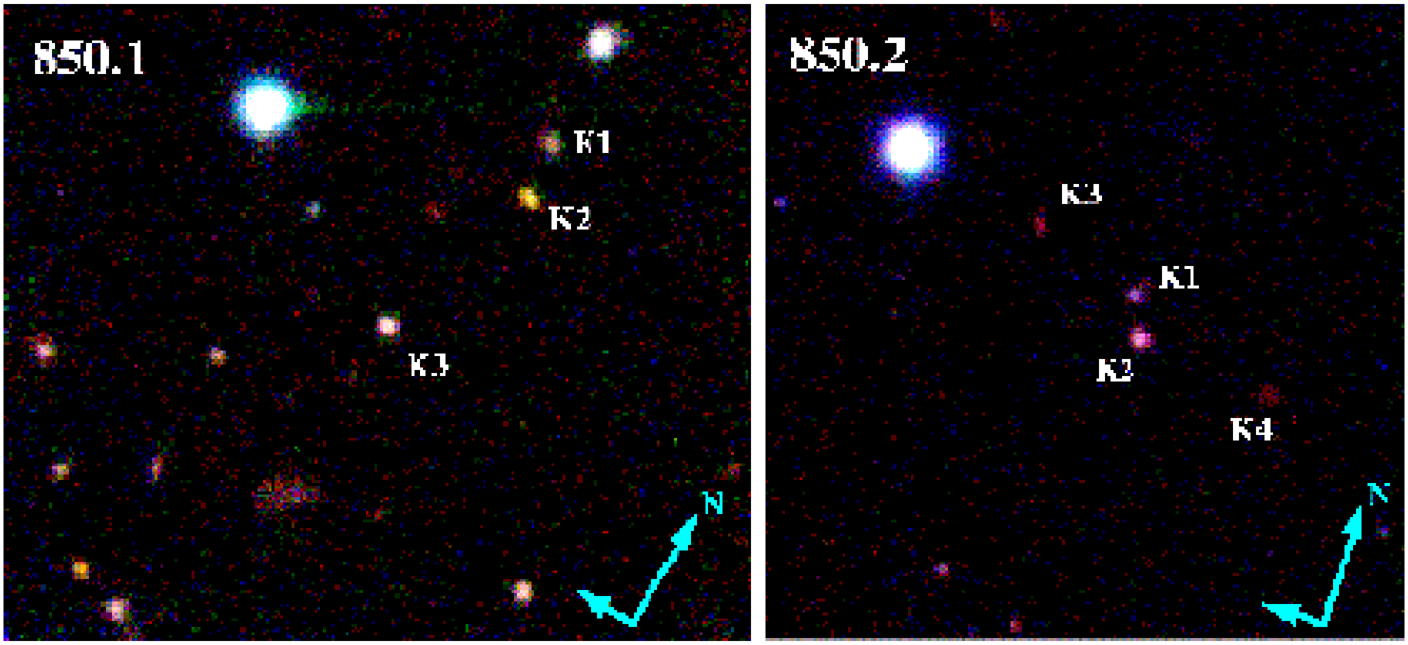

FIG. 3.— Composite color images of the fields of HzRG850.1 and HzRG850.2, constructed from the Keck *JHK* imaging. We label the possible candidate counterparts to the submm sources as well as several other sources in the close vicinity. The field of HzRG850.1 is $54'' \times 47''$, while HzRG850.2 is $47''$ square. Orientations are shown.

for their classification, analogous to that used for proto-stars, and building upon the evolutionary scheme for ULIRGs proposed by Sanders et al. (1988). For operational purposes we base this scheme on the typical depths achieved in follow-up observations ($I \sim 26$, $K \sim 21$) and the properties of the submm galaxies discussed in Ivison et al. (1998, 2000), Hughes et al. (1998), Smail et al. (1999) and Soucail et al. (1999). We define the following classes: Class 0, very-highly obscured sources, where there is no plausible optical or near-IR counterpart; Class I, highly obscured sources, where only a near-IR counterpart exists (often EROs — Elston, Rieke & Rieke 1988; Dey et al. 1999; Smail et al. 1999); and Class II, where an obvious optical counterpart is seen (IIa: pure starburst; IIb: type-II AGN; IIc: type-I AGN). The latter class may overlap with the most massive examples of Lyman-break-selected objects (Adelberger & Steidel 2000). We note that Classes 0 and I may also include sources which are fainter in the optical/near-IR by virtue of being at higher redshifts; however, for the purposes of the discussion here we assume that the different classifications arise solely from differences in the obscuration of the sources.

Turning to the optical and near-IR imaging of this field, we start by discussing HzRG850.1. There are three possible optical or near-IR counterparts to this source lying within or near the 450- and 850-μm errors circles (Figs. 2 & 3; see also Table 2). The bluest of these sources is 850.1.K1 (Class II), which falls within the 450-μm error circle. Lacy & Rawlings (1996) detect this source in the U-band ($U-V \sim -0.9$; LR3 in their paper) and we therefore conclude that 850.1.K1 is probably a low-redshift, blue galaxy and unlikely to be associated with the SCUBA source. The remaining two galaxies, 850.1.K2 and 850.1.K3 (both Class I) have similar very red colors, $V-K \sim 7$, with 850.1.K2 falling within both the 850-μm and 450-μm error circles. The similar, very red colors of 850.1.K2 and 850.1.K3 (Fig. 3; Table 2), combined with the fact that the 850-μm source HzRG850.1 is spatially extended, suggests that both these galaxies may be jointly responsible for the submm emission. We also note some *very* faint emission in V and K to the west of 850.1.K2, and in V alone to the south.

For HzRG850.2, three faint galaxies are visible in the K image (Figs. 2 & 3): the bluer of these, 850.2.K1, lies just within the error ellipse, while the others, 850.2.K2 and 850.2.K3, are much redder, $R-K \geq 6.4$, and lie on the edge of the nominal error ellipse. In the deep *HST* WFPC2 F702W image, both 850.2.K1 and 850.2.K2 are each resolved into two components, while 850.2.K3 is undetected ($R > 26$, 3σ). For 850.2.K1 the sub-components both appear to be galaxies, while in 850.2.K2 they may either be two galaxies or a single system crossed by a dust lane. As with HzRG850.1, it is plausible that both of these counterparts may be contributing to the submm emission from HzRG850.2, given its morphology (Fig. 1).

TABLE 2
CANDIDATE NEAR-IR IDENTIFICATIONS FOR SUBMM SOURCES

ID	R.A. (J2000)	Dec. (J2000)	K	$V-K$	$R-K$
850.1.K1	06 50 51.12	+41 30 09.2	20.0±0.4	4.5±0.4	...
850.1.K2	06 50 51.05	+41 30 06.8	19.0±0.2	7.0±0.3	...
850.1.K3	06 50 51.29	+41 29 58.6	19.4±0.3	6.9±0.3	...
850.2.K1	06 50 49.14	+41 31 25.6	19.6±0.3	4.6±0.3	4.4±0.3
850.2.K2	06 50 49.07	+41 31 23.7	19.2±0.2	7.4±0.4	6.4±0.2
850.2.K3	06 50 49.71	+41 31 28.2	20.2±0.4	5σ >6.1	$5\sigma > 5.3$
850.3	...	...	$5\sigma > 20.0$	...	...
850.4.K1	06 50 53.95	+41 29 40.4	20.5±0.5	...	5σ >5.6
850.5	...	...	$5\sigma > 20.0$	...	...

HzRG850.3 unfortunately lies in a region where the K-band imaging is relatively shallow (Fig. 2). No obvious counterpart is visible in the KPNO K-band image down to $K = 19.8$ (3σ). There is, however, a very faint $V \gtrsim 27$ source visible within the 850-μm error circle. In addition, there are a pair of faint ($V \sim 25.6$, 26.0) galaxies that lie $\sim 5.6''$ northeast of the SCUBA source centroid. However, the faintness of these galaxies and the lack of any useful color information renders it difficult to place much confidence in these galaxies as likely candidates for the submm emission. We conclude that HzRG850.3 must either be a Class 0 or I submm galaxy.

The remaining SCUBA sources lie in comparatively shallow regions of the near-IR and optical images and do not show unambiguous identifications. HzRG850.4 has a very faint ($K \sim 20.5$) and extended counterpart (850.4.K1) visible in the

K-band image within the 850-μm error circle (Fig. 2). The position of 850.4.K1 in the V-band image is contaminated by the diffraction spike from a bright star, but there is no obvious counterpart to this source visible in the deep *HST* F702W image and we conclude that it is a Class I source. For HzRG850.5 there are no obvious sources visible in the K or F702W image (Class 0 or I), and the V-band image is again contaminated by the nearby star.

In summary, HzRG850.1 and HzRG850.2 are likely to be associated with EROs (i.e. Class I sources). HzRG850.3 and HzRG850.4 may be associated with very faint galaxies, and HzRG850.5 has no obvious counterpart (Class 0 or I). It is interesting that our success in obtaining candidate identifications, in particular the association with EROs, correlates with the observed flux density of the submm emission. Is it possible that the brightest submm sources are typically associated with Class I or II counterparts (e.g. HR10, Dey et al. 1999; SMM J09429+4658, Smail et al. 1999; SMM J02399–0136, Ivison et al. 1998; SMM J14011+0252, Ivison et al. 2000) whereas fainter submm sources typically have Class 0 counterparts (see also Hughes et al. 1998; Smail et al. 2000).

3.4. *Redshift constraints*

Finally, we discuss whether the submm sources can be unambiguously placed at high redshifts, $z \gg 1$, and hence whether we can strengthen the case for their association with 4C 41.17. In the absence of deep spectroscopy of the counterparts discussed in §3.3, we are reliant on other redshift-sensitive parameters. Two examples are: *a*) the 450- to 850-μm flux ratio, which falls steadily as the peak of the dust SED shifts through the 450-μm filter at increasing redshift; and *b*) the 850-μm to 1.4-GHz flux ratio, based upon the local far-IR/radio correlation for star-forming galaxies, is a robust redshift indicator where $F_\nu \propto \nu^{+3.5}$ at submm wavelengths, while $F_\nu \propto \nu^{-0.7}$ in the radio, yielding a flux ratio that rises initially as $(1+z)^{+4.2}$ (Carilli & Yun 1999, 2000; Blain 1999; see also Smail et al. 2000).

Dealing with the 450- to 850-μm flux ratio first, the observed ratios for 4C 41.17 and HzRG850.1 are 3.2 ± 0.8 and 2.2 ± 0.6, consistent with their being at the same redshift, with best-fit values and ranges of $z \sim 3.8$ ($2.8 < z < 5.1$) and ~ 4.8 ($3.5 < z < 6.1$), respectively, based on extreme models of starbursts (Hughes et al. 1998). These limits are supported by constraints from the 850-μm to 1.4-GHz flux ratio. For HzRG850.1, where $S_{850\mu\mathrm{m}}/S_{1.4\mathrm{GHz}} \geq 180$ (taking radio limits of $3\sigma < 90\,\mu$Jy from the re-reduced radio image published originally by Carilli, Owen & Harris 1994), we arrive at a robust limit of $z \geq 2$. The limits for HzRG850.2 and HzRG850.3 are slightly weaker, but they are certainly not local galaxies.

The extreme colors, $V - K \sim 7$, of the probable galaxy counterparts to HzRG850.1 and HzRG850.2, as well as the faintness of the counterparts to the remaining sources, suggests that these systems also lie at high redshifts. The K-band magnitudes for the candidate identifications quoted are fairly bright: if these galaxies do lie at $z = 3.8$ then they are very luminous, in excess of $50L^*$, although we note that luminosities close to this are found for the confirmed Class II counterparts SMM J02399–0136 ($z = 2.8$, Ivison et al. 1998) and SMM J14011+0252 ($z = 2.6$, Ivison et al. 2000).

We conclude that the available constraints suggest that the over-density of bright submm galaxies identified in the 4C 41.17 field is likely to lie at $z > 2.8$ and hence is consistent with being associated with the radio galaxy at $z = 3.8$ (though spectroscopic confirmation is clearly a top priority). This suggests that in addition to the proposed over-density of Lyman-break galaxies identified around 4C 41.17 by Lacy & Rawlings (1996), we should also add a comparably numerous population of highly-obscured and very luminous submm galaxies.

4. CONCLUSIONS

We report the discovery of five new luminous submm sources within a 2.5′-diameter (1 Mpc at $z = 3.8$) area centered on the submm-bright $z = 3.8$ radio galaxy, 4C 41.17. Three of these sources are as bright or brighter than any other known blank-field submm galaxies. This surface density of submm galaxies is an order of magnitude greater than that expected from blank-field counts: we would need to map at least 600 blank fields to find a chance configuration of such bright sources. Using the available constraints, we suggest that this over-density lies at $z > 2.8$ and is therefore consistent with a structure associated with 4C 41.17.

We note that this field exhibits an over-density above that expected in blank fields, not only at submm wavelengths, but also in samples of galaxies selected via the Lyman-break technique (Lacy & Rawlings 1996) and for their extremely red colors (EROs). As many as five of the latter class of galaxies may be directly associated with the luminous submm sources seen in this field.

We introduce a classification scheme for the counterparts of submm sources, based upon observations of well-studied SCUBA galaxies. Within the framework of this scheme we propose that submm galaxies and ERO starbursts represent different aspects of a single evolutionary cycle. Following on from this, we suggest that the over-densities of both the submm and ERO populations in this field represent young, dusty starbursts forming within a proto-cluster centered on the radio galaxy at $z = 3.8$, which also hosts a population of less-obscured Lyman-break galaxies.

More observations are clearly needed to confirm the nature of this over-density, to test our suggestion that it is associated with the radio source at $z = 3.8$ and, most interestingly, to investigate if it represents a virialised structure. The most feasible test of the latter issue will be to image this field using the *Chandra* or *Newton* X-ray observatories to identify emission from the hot intracluster medium confined within the potential well of the proposed proto-cluster.

We are currently expanding our survey to cover 15 fields centered on HzRGs to determine more reliable limits on the prevalence of similar over-densities of submm sources around massive galaxies at high redshifts, $z = 3$–5.

ACKNOWLEDGEMENTS

We thank Chris Carilli and Wil van Breugel for providing their Very Large Array and *HST* images of the 4C 41.17 field, Dr F. Chaffee for assistance with obtaining the V-band image, Gary Punawai and Greg Wirth for their expert assistance at the W. M. Keck Observatory, as well as H. Halbedel, G. MacDougal, C. Snedden, H. Schweiker and G. Tiede for their expert assistance at the KPNO 2.1m. We are grateful to the referee, Chris Carilli, for suggestions that improved this paper markedly. The JCMT is operated by the Joint Astronomy Centre on behalf of the United Kingdom Particle Physics and Astronomy Research Council (PPARC), the Netherlands Organisation for Scientific Research, and the National Research Council of Canada. KPNO is a division of the National Optical Astronomy Observatory, which is operated by the AURA, under cooperative agreement with the NSF. The W. M. Keck Observatory is operated as a scientific partnership among the California Institute of Technology, the University of California and NASA.

REFERENCES

Adelberger, K. L., & Steidel, C. C. 2000, ApJ, submitted (astro-ph/0001126)
Aragón-Salamanca, A., Ellis, R. S., Couch, W. J., & Carter, D. 1993, MNRAS, 262, 764
Aragón-Salamanca, A., Ellis, R. S., Schwartzenberg, J.-M., & Bergeron, J. A. 1994, ApJ, 421, 21
Barger, A. J., Cowie, L. L., Sanders, D. B., Fulton, E., Taniguchi, Y., Sato, Y., Kawara, K., & Okuda, H. 1998, Nature, 394, 248
Barger, A. J., Cowie, L. L., & Sanders, D. B. 1999, ApJ, 518, L5
Baron, E., & White, S. D. M. 1987, ApJ, 322, 585
Baugh, C. M., Benson, A. J., Cole, S., Frenk, C. S., & Lacey, C. G. 1999, MNRAS, 305, L21
Blain, A. W. 1999, MNRAS, 309, 955
Blain, A. W., & Longair, M. S. 1993, MNRAS, 264, 509
Blain, A. W., Kneib, J.-P., Ivison, R. J., & Smail, I. 1999, ApJ, 512, L87
Bower, R. G., Lucey, J. R., & Ellis, R. S. 1992, MNRAS, 254, 601
Carilli, C. L., Owen, F. N., & Harris, D. E. 1994, AJ, 107, 480
Carilli, C. L., Röttgering, H., van Ojik, R., Miley, G., & van Breugel, W. J. M. 1997, ApJS, 109, 1
Carilli, C. L., Harris, D. E., Pentericci, L., Röttgering, H., Miley, G., & Bremer, M. N. 1998, ApJ, 496, L57
Carilli, C. L., & Yun, M. S. 1999, ApJ, 513, L13
Carilli, C. L., & Yun, M. S. 2000, ApJ, 530, 618
Chambers, K. C., Miley, G. K. & van Breugel, W. J. M. 1990, ApJ, 363, 21
Cole, S. M., Aragon-Salamanca, A., Frenk, C. S., Navarro, J. F., & Zepf, S. E. 1994, MNRAS, 271, 781
Dey, A., Spinrad, H., & Dickinson, M. E. 1995, ApJ, 440, 515
Dey, A. 1999, in The Most Distant Radio Galaxies, Proc. of the Royal Netherland Academy of Arts & Sciences, ed. H. J. A. Rottgering, P. A. Best, & M. D. Lehnert, p. 12
Dey, A., Graham, J. R., Ivison, R. J., Smail, I., Wright, G. S., & Liu, M. C. 1999, ApJ, 519, 610
Dunlop, J. S., Hughes, D. H., Rawlings, S., Eales, S. A., & Ward, M. J. 1994, Nature, 370, 347
Eales, S., Lilly, S., Gear, W., Dunne, L., Bond, J. R., Hammer, F., Le Fèvre, O., & Crampton, D. 1999, ApJ, 515, 518
Efstathiou, G., & Rees, M. 1988, MNRAS, 230, P5
Ellis, R. S., Smail, I., Dressler, A., Couch, W. J., Oemler, A. Jr., Butcher, H., & Sharples, R. M. 1997, ApJ, 483, 582
Elston, R., Rieke, G. H., & Rieke, M. J. 1988, ApJ, 331, L77
Fixsen, D. J., Dwek, E., Mather, J. C., Bennett, C. L., & Shafer, R. A. 1998, ApJ, 508 123
Graham, J. R., Matthews, K., Soifer, B. T., Nelson, J. E., Harrison, W., Jernigan, J. G., Lin, S., Neugebauer, G., Smith, G., & Ziomkowski, C. 1994, ApJ, 420, L5
Hogbom, J. A. 1974, A&AS, 15, 417
Holland, W. S., et al. 1999, MNRAS, 303, 659
Hughes, D. H., et al. 1998, Nature, 394, 241
Ivison, R. J., Smail, I., Le Borgne, J.-F., Blain, A. W., Kneib, J.-P., Bézecourt, J., Kerr, T. H., & Davies, J. K. 1998, MNRAS, 298, 583
Ivison, R. J., Smail, I., Barger, A. W., Kneib, J.-P., Blain, A. W., Owen, F. N., Kerr, T. H., & Cowie L. L. 2000, MNRAS, in press (astro-ph/9911069)
Jenkins, A., Colerg, J. M., Frenk, C. S., Evrard, A. E., White, S. D. M., Yoshida, N., & Cole, S. M. 2000, MNRAS, in press
Jenness, T., & Lightfoot, J. F. 1998, in ASP Conf. Ser. 145, Astronomical Data Analysis Software and Systems VII, ed. R. Albrecht, et al. (San Francisco: ASP), 216
Kaiser, N. 1984, ApJ, 284, L9
Kauffmann, G., & Charlot, S. 1998, MNRAS, 294, 705
Kauffmann, G., Colberg, J. M., Diaferio, A., & White, S. D. M. 1999, MNRAS, 303, 188
Lacy, M. & Rawlings, S. 1996, MNRAS, 280, 888
Lilly, S. J., & Longair, M. S. 1984, MNRAS, 211, 833
Lilly, S. J., Eales, S. A., Gear, W. K. P., Hammer, F., Le Fèvre, O., Crampton, D., Bond, J. R., & Dunne, L. 1999, ApJ, 518, 641
Liu, M. C., Dey, A., Graham, J. R., Bundy, K. A., Steidel, C. C., Adelberger, K. L., & Dickinson, M. E. 2000, ApJ, in press (astro-ph/0002443)
Matthews, T. A., Morgan, W. W., & Schmidt, M. 1964, ApJ, 140, 35
Matthews, K., & Soifer, B. T. 1994, in: Infrared Astronomy with Arrays: the Next Generation, ed. I. McLean, (Dordrecht: Kluwer), 239
McLure, R. J., Dunlop, J. S., Kukula, M. J., Baum, S. A., O'Dea, C. P., & Hughes, D. H. 1999, MNRAS, 308, 377
Oke, J. B., et al. 1995, PASP, 107, 375
Pentericci, L., Röttgering, H. J. A., Miley, G. K., Spinrad, H., McCarthy, P. J., van Breugel, W. J. M., & Macchetto, F. 1998, ApJ, 504, 139
Persson, S. E., Murphy, D. C., Krzeminski, W., Roth, M., & Rieke, M. J. 1998, AJ, 116, 2475
Rosati, P., Stanford, S. A., Eisenhardt, P. R., Elston, R., Spinrad, H., Stern, D., & Dey, A. 1999, AJ, 118, 76
Sanders, D. B., & Mirabel, I. F. 1996, ARAA, 34, 749
Sanders, D. B., Soifer, B. T., Elias, J. H., Madore, B. F., Matthews, K., Neugebauer, G., & Scoville, N. Z. 1988, ApJ, 325, 74
Smail, I., Ivison, R. J., & Blain, A. W. 1997, ApJ, 490, L5
Smail, I., Ivison, R. J., Kneib, J.-P., Cowie, L. L., Blain, A. W., Barger, A. J., Owen, F. N., & Morrison, G. 1999, MNRAS, 308, 1061
Smail, I., Ivison, R. J., Owen, F. N., Blain, A. W., & Kneib, J.-P. 2000, ApJ, 528, 612
Soucail, G., Kneib, J.-P., Bézecourt, J., Metcalfe, L., Altieri, B., & Le Borgne, J.-F. 1999, A&A, 343, L70
Stanford, S. A., Elston, R., Eisenhardt, P. R., Spinrad, H., Stern, D., & Dey, A. 1997, AJ, 114, 2232
Stanford, S. A., Eisenhardt, P. R., & Dickinson, M. 1998, ApJ, 492, 461
Steidel, C. C., Pettini, M. & Hamilton, D. 1995, AJ, 110, 2519
Steidel, C. C., Adelberger, K. L., Giavalisco, M., Dickinson, M., & Pettini, M. 1999, ApJ, 519, 1
Thompson, D., Beckwith, S. V. W., Fockenbrock, R., Fried, J., Hippelein, H., Huang, J.-S., von Kuhlmann, B., Leinert, C., Meisenheimer, K., Phleps, S., Roser, H.-J., Thommes, E., & Wolf, C. 1999, ApJ, 523, 100
van Breugel, W. J. M., Stanford, S. A., Spinrad, H., Stern, D., & Graham, J. R. 1998, ApJ, 502, 614
White, S. D. M., & Frenk, C. S. 1991, ApJ, 379, 52
Yamada, T., Tanaka, I., Aragón-Salamanca, A., Kodama, T., Ohta, K., & Arimoto, N. 1997, ApJ, 487, L125
Zirm, A., Dey, A., Dickinson, M., McCarthy, P. J., Eisenhardt, P., Djorgovski, S. G., Spinrad, H., Stanford, S. A., & van Breugel, W. 2000, in ASP Conf. Ser. 193, The Hy-Redshift Universe: Galaxy Formation and Evolution at High Redshift, ed. A. J. Bunker, & W. J. M. van Breugel (San Francisco: ASP), 114